JOURNAL OF NATURAL PRODUCTS

Note

pubs.acs.org/jnp

Unambiguous Determination of the Absolute Configuration of Dimeric Stilbene Glucosides from the Rhizomes of *Gnetum africanum*

Thierry Buffeteau,*[,‡] Dominique Cavagnat,[‡] Jonathan Bisson,[†] Axel Marchal,[§] Gilbert D. Kapche,[†] Ilaria Battistini,[†] Gregory Da Costa,[†] Alain Badoc,[†] Jean-Pierre Monti,[†] Jean-Michel Mérillon,[†] and Pierre Waffo-Téguo*[,†]

[†]Groupe d'Etude des Substances Végétales à Activité Biologique, EA 3675, Université Bordeaux, ISVV, 210 Chemin de Leysotte, F-33882 Villenave d'Ornon, France

[‡]Institut des Sciences Moléculaires, UMR 5255−CNRS, Université Bordeaux, 351 Cours de la Libération, F-33405 Talence, France

[§]Unité de Recherche Œnologie, EA 4577, INRA USC 1366, Université Bordeaux, ISVV, 210 Chemin de Leysotte, F-33882 Villenave d'Ornon, France

Supporting Information

ABSTRACT: Dimeric stilbene glucosides **1**−**3** [two diastereomers of (−)-gnemonoside A (**1a** and **1b**), (−)-gnemonoside C (**2**), and (−)-gnemonoside D (**3**)] as well as a mixture of the two enantiomers of gnetin C (**4**) were isolated from the rhizomes of *Gnetum africanum*. The two enantiomers of gnetin C, (+)-**4** and (−)-**4**, were obtained from the aglycones of **1a** and **1b**, respectively. The configurations of these stilbenoids were investigated by NMR and vibrational circular dichroism (VCD) experiments. The absolute configurations of (−)-**1a**, (−)-**2**, (−)-**3**, and (−)-**4** were established as 7a*S*,8a*S* by VCD spectroscopy in combination with density functional theory calculations. The antiamyloidogenic activity of the isolated stilbenes was also evaluated versus beta-amyloid fibrils. The four glucosides of gnetin C (**1a**, **1b**, **2**, and **3**) were found to be the most active compounds, with inhibition percentages of 56, 56, 58, and 54 at 10 μM, respectively.

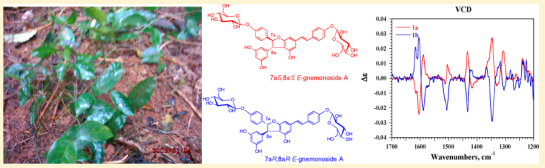

Gnetum africanum Welw. (Gnetaceae) is distributed and cultivated in humid tropical forests in the west central Africa region.[1] In Cameroon, it is known as Eru or Okok.[2] Parts of this plant are used as folk medicine for the treatment of enlarged spleen and sore throat and as a cathartic and are considered to be an antidote to some forms of poison.[3] The leaves are used as a dressing for warts and boils, while a tisane of the cut-up stem is taken to reduce the pain of childbirth.[3] Eaten raw or finely shredded and added to soups and stews, it is considered to have high nutritional value and is an important source of protein, essential amino acids, and minerals.[3,4]

Stilbenoids, a family of phenolic compounds, occur with a limited distribution in the plant kingdom, mainly in families such as the Vitaceae, Dipterocarpaceae, Fabaceae, and Gnetaceae. Numerous oligostilbenoids have been isolated from the Gnetaceae.[5−9] They are structurally derived from 1,2-diphenylethene. A large array of compounds share this simple skeleton.[8] The variety and complexity of configuration of the oligomers, which result from the oxidative coupling of the monomers, add to their diversity. The stereochemical complexity of these molecules also increases with their degree of polymerization. The five-membered oxygen heterocycle (1,2-diaryldihydrobenzofuran moiety) bearing *trans*-oriented aryl rings is the most important framework in the oligostilbenes found in the Gnetaceae. These polyphenols have been shown to have diverse biological activities. Resveratrol, the most widely studied stilbenoid, has been shown to have a variety of activities such as cancer chemoprevention[10] and neuroprotective activity.[11] In a previous study, we showed that *E*-ε-viniferin glucoside, a dimeric resveratrol glucoside isolated from the grapevine, strongly inhibited in vitro the fibril formation of the peptide Aβ,[12] a pathologic agent likely involved in Alzheimer's disease. It also had a strong protective effect against peptide Aβ-induced PC12 cell death.[13]

In our continuing search for neuroprotective stilbenoids, four dimeric stilbene glucosides, **1a**, **1b**, **2**, and **3**, as well as a mixture of the two enantiomers of gnetin C [(+)-**4** and (−)-**4**] were isolated from the rhizomes of *G. africanum* (Figure 1). These molecules share with ε-viniferin the 1,2-diaryldihydrobenzofuran moiety, but their configurations have not yet been determined. This study aimed at answering two questions arising from chemical characterization performed on these compounds. First, what is the structural difference between **1a** and **1b**, which have the same mass and similar NMR spectra? Second, what are the absolute configurations of (+)- and (−)-gnetin C? To answer these questions, we had to determine the absolute configuration of the C-7a and C-8a stereogenic carbons of the dihydrobenzofuran ring of these stilbenoids. As crystallization attempts were unsuccessful, vibrational circular dichroism (VCD) and comparison of experimental results with

Received: May 26, 2014

dx.doi.org/10.1021/np500427v | *J. Nat. Prod.* XXXX, XXX, XXX−XXX

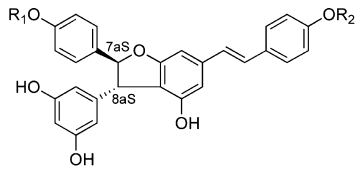

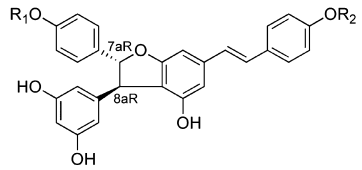

	C-7a	C-8a	R_1	R_2
(−)-*E*-gnemonoside A (**1a**)	*S*	*S*	β-D-Glc	β-D-Glc
(−)-*E*-gnemonoside A (**1b**)	*R*	*R*	β-D-Glc	β-D-Glc
(−)-*E*-gnemonoside C (**2**)	*S*	*S*	β-D-Glc	H
(−)-*E*-gnemonoside D (**3**)	*S*	*S*	H	β-D-Glc
(+)-*E*-gnetin C [(+)-**4**]	*R*	*R*	H	H
(−)-*E*-gnetin C [(−)-**4**]	*S*	*S*	H	H

Figure 1. Chemical structures of isolated compounds.

calculated spectra based on density functional theory (DFT) were employed.[14−17]

Compounds **1**−**4** were isolated from the rhizomes of *G. africanum*. Compound **1** was obtained from the aqueous extract (**GaA**), whereas compounds **2**−**4** were obtained from the organic extract (**GaM**). The ^{1}H and ^{13}C NMR data of compounds **2**−**4** (see Supporting Information, Table S1) were similar to reported data for gnemonoside C, gnemonoside D, and gnetin C, respectively.[18]

To enhance the stilbenoid content, the aqueous-soluble partition (**GaA**) was prepurified on Amberlite XAD-7 (H_2O and acetone), using the previously published protocol.[19] This provided a semipurified extract enriched in the target molecules **1a** and **1b**. Negative LC-ESI-FTMS spectra of compounds **1a** and **1b** showed similar molecular $[M - H]^-$ ions at *m/z* 777.2401 and 777.2402, respectively, in agreement with the molecular formula of $C_{40}H_{42}O_{16}$. Their full-scan FTMS spectra were indistinguishable, exhibiting source fragment ions at *m/z* 615.1874/615.1875 and 453.1346/453.1347 (Supporting Information, Figure S1). These ions correspond to formulas $C_{34}H_{31}O_{11}$ (loss of one hexose moiety) and $C_{28}H_{21}O_6$ (loss of two hexose moieties), respectively. The ^{1}H NMR, ^{1}H−^{1}H COSY, ^{1}H−^{1}H ROESY, HSQC, and HMBC spectra of **1a** are reported in the Supporting Information (Figures S2−S6). The ^{1}H and ^{13}C NMR spectra (Supporting Information, Table S1) of the two compounds were superimposable, suggesting that the structures of **1a** and **1b** were similar. These NMR spectra were also found to be similar to the spectra reported for gnemonoside A.[18]

VCD experiments were performed to determine the configurations of these stilbenoids. VCD spectra of **1a** and **1b** were recorded in DMSO-d_6 at a concentration of 50 mM and are reported in Figure 2. The two spectra are not perfectly opposite with respect to the baseline, revealing that the two molecules are not enantiomers, but could be diastereomers. Indeed, since the glucopyranosyl (Glc) groups have the same chirality (*β*-D-Glc) in both **1a** and **1b**, these compounds are diastereoisomers.

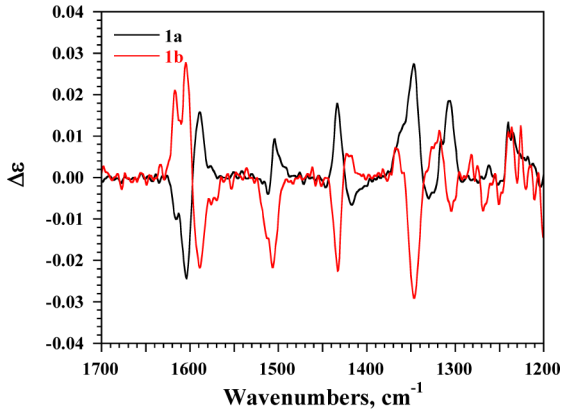

Figure 2. Experimental VCD spectra of **1a** and **1b** in DMSO-d_6 solution (50 mM, 100 *μ*m path length).

To confirm this assumption, we had to show that the aglycones of **1a** and **1b** are enantiomers. Upon enzymatic hydrolysis with *β*-glucosidase,[20] compounds **1a** and **1b** gave aglycones that coeluted in HPLC. These two new compounds had opposite optical rotations (−17 and +20 for the aglycones of **1a** and **1b**, respectively) and opposite VCD spectra as shown in Figure 3. Thus, the aglycones of **1a** and **1b** correspond to the two enantiomers of gnetin C, (−)-**4** and (+)-**4**, respectively.

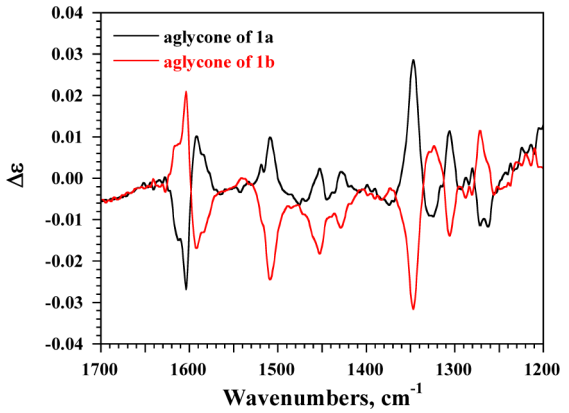

Figure 3. Experimental VCD spectra of aglycones of **1a** and **1b** in DMSO-d_6 solution (50 mM, 100 *μ*m path length).

Theoretical calculations were performed to determine the absolute configuration of (−)-**4**. The conformational analysis of (7a*S*,8a*S*)- and (7a*R*,8a*S*)-gnetin C was carried out initially by using semiempirical RM1 calculations with the simulated annealing technique. A *trans*-configured olefinic bond was used. Twenty conformers for (7a*S*,8a*S*)- and (7a*R*,8a*S*)-gnetin C with energies within 2.4 kJ/mol of the lowest energy conformer were kept. Subsequently, the 20 RM1 conformations of (7a*S*,8a*S*)- and (7a*R*,8a*S*)-gnetin C were optimized by using DFT at the B3PW91/6-31G** level. Calculations were performed for the isolated molecule in vacuo. Harmonic vibrational frequencies were calculated at the same level to confirm that all structures were stable conformations and to enable free energies to be calculated. The predicted VCD spectrum, taking into account the relative populations of (7a*S*,8a*S*)- and (7a*R*,8a*S*)-gnetin C, was compared to the experimental spectrum of (−)-**4** in Figure 4. The predicted VCD spectra of (7a*S*,8a*S*)- and (7a*R*,8a*S*)-gnetin C isomers reproduced fairly well the intensity and the sign of most bands

dx.doi.org/10.1021/np500427v | *J. Nat. Prod.* XXXX, XXX, XXX−XXX

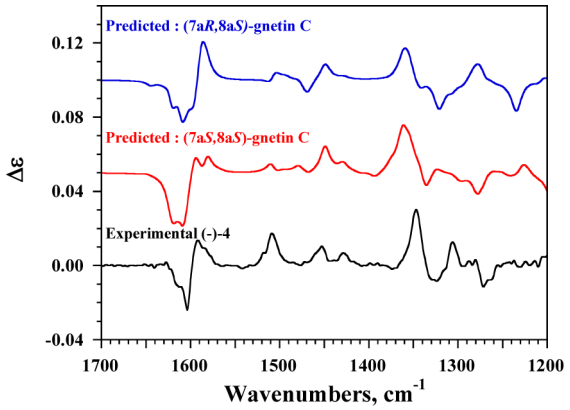

Figure 4. Comparison of experimental VCD spectrum for the aglycone of **1a** [i.e., (−)-**4**] recorded in DMSO-d_6 solution (50 mM, 100 μm path length) with the predicted VCD spectrum of (7a*S*,8a*S*)- and (7a*R*,8a*S*)-gnetin C isomers.

observed in the experimental spectrum, allowing the definitive determination of the 8a*S* configuration. The determination of the configuration of the C-7a stereogenic carbon was less obvious from VCD data, even though a better agreement between theoretical and experimental spectra was obtained for the 7a*S* configuration [predicted spectra of (7a*S*,8a*S*)-gnetin C]. The 7a*S* configuration was confirmed by the absence of a cross-peak between H-7a (δ = 5.32) and H-8a (δ = 4.35) in the ROESY spectrum (Supporting Information, Figure S4), indicating the opposite facial orientation of these two protons. Thus, this VCD analysis, associated with NMR results, unambiguously established the 7a*S*,8a*S* configuration of (−)-**4**. In turn, the (7a*R*,8a*R*)-(+)-gnetin C isomer corresponds to the aglycone of **1b**.

The VCD spectrum of natural gnetin C (**4**) was also recorded in DMSO-d_6 at a concentration of 50 mM and is shown in Figure 5. The signs of the different VCD bands were

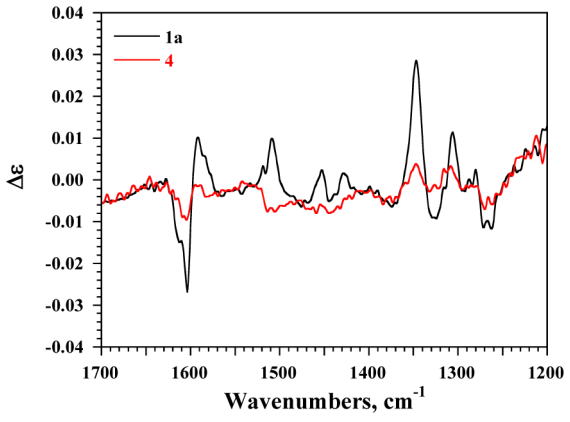

Figure 5. Comparison of experimental VCD spectra of the aglycone of **1a** and natural gnetin C (**4**) in DMSO-d_6 solution (50 mM, 100 μm path length).

the same as those observed for the aglycone of **1a**, but their intensities were significantly lower by almost 5-fold. This indicated that the 7a*S*,8a*S* enantiomer of gnetin C is slightly preponderant in natural gnetin C isolated from *G. africanum* with an enantiomeric excess lower than 20%. Interestingly, all the bands observed in the VCD spectra of **2** and **3** had the same sign as that for compound **1a**, but their intensities were slightly lower (Supporting Information, Figure S7). The 7a*S*,8a*S* configuration of the benzofuran moiety was preserved for the stilbene dimer glucosides **1a**, **2**, and **3**.

Compounds **1a**, **1b**, **2**, **3**, and **4** were evaluated for their antiamyloidogenic activities. The assay was performed as previously described.[21] As shown in Table 1, compound **4**

Table 1. Inhibition of Aβ (25-35) Fibril Formation at 10 μM

compound	% inhibition Aβ (25−35)
curcumin	53 ± 5
1a and **1b**	56 ± 2
2	58 ± 7
3	54 ± 2
4	39 ± 5

(gnetin C) was marginally active, with 39% inhibition of the aggregation of β-amyloid peptide, whereas its four glucosides, **1a**, **1b**, **2**, and **3**, were the most active compounds with 56%, 56%, 58%, and 54% inhibition at 10 μM, respectively. These compounds may provide insights into the implication of Aβ fibril formation in Alzheimer's disease and could serve as precursors for the development of aggregation-inhibition therapies. Futhermore, knowledge of the absolute configurations and the enantiomeric purities of the samples could help in understanding their biological activities.

In this study, we reported the absolute configuration of four stilbene dimer glucosides extracted from the rhizomes of *G. africanum* using VCD and NMR spectroscopy experiments. The hydrolysis of the two diastereomers of (−)-gnemonoside A (**1a** and **1b**) permitted the first definition of the absolute configurations of the two enantiomers of gnetin C as 7a*S*,8a*S* for (−)-*E*-gnetin C and 7a*R*,8a*R* for (+)-*E*-gnetin C. This study also shows that the 7a*S*,8a*S* enantiomer is slightly preponderant in natural gnetin C extracted from *G. africanum* with an enantiomeric excess lower than 20%.

EXPERIMENTAL SECTION

General Experimental Procedures. ^{1}H and ^{13}C NMR spectra were recorded on a Bruker Avance III 600 MHz NMR spectrometer and analyzed with Bruker Topspin software. Compounds were measured in 3 mm NMR tubes, using methanol-d_4 as the solvent. The optical rotations were measured in MeOH at 20 °C on a JASCO P-2000 polarimeter using the sodium emission wavelength (λ = 589 nm). The centrifugal partition chromatography (CPC) (FCPC200) was provided by Kromaton Technologies (Sainte-Gemmes-sur-Loire, France). The solvents were pumped by a Gilson 321-H1 two-way binary high-pressure gradient pump. The samples were introduced into the CPC column via a high-pressure injection valve (3725i-038 Rheodyne) equipped with a 20 mL sample loop. The CPC fractions were monitored with a Varian Prostar 325 DAD detector (Victoria, Australia), at wavelengths of 306 and 280 nm. HPLC preparative separations were carried out using a Varian Prostar 345 UV−visible detector and a binary pump with a Varian Dynamax Microsorb 100-5 C_{18} (10 μm, 250 × 21.4 mm) column. The mobile phase was composed of two solvents: (A) 0.025% TFA in H_2O and (B) MeCN. LC-FTMS analysis was carried out using an HTC PAL autosampler (CTC Analytics AG, Zwingen, Switzerland), an Accela U-HPLC system with quaternary pumps, and an Exactive benchtop Orbitrap mass spectrometer equipped with a heated electrospray ionization (HESI) probe (both from Thermo Fisher Scientific, Bremen, Germany). External mass calibration was performed with Pierce ESI negative and positive ion calibration solution (Thermo Fisher Scientific). For liquid chromatography separation, a C_{18} column was used as the stationary phase (Acquity BEH 2.1 mm × 150 mm, 1.7 μm particle size, Waters SA, Wexford, Ireland). The mobile phases were

dx.doi.org/10.1021/np500427v | *J. Nat. Prod.* XXXX, XXX, XXX−XXX

(A) water + 0.1% formic acid and (B) MeCN. The flow rate was 400 μL/min, and eluent B varied as follows: 0 min, 15%; 0.5 min, 15%; 6.5 min, 35%; 6.6 min, 98%; 8.5 min, 98%; 8.6 min, 15%; 10 min, 15%. The injection volume was 5 μL. Mass acquisitions were carried out in negative Fourier transform mass spectrometry (FTMS) ionization mode at a unit resolution of 50 000 ($m/\Delta m$, fwhm at 200 amu). The sheath and auxiliary gas flows (both N_2) were optimized at 75 and 18 arbitrary units, respectively. The HESI probe and capillary temperatures were 320 and 350 °C, respectively. The electrospray voltage was set to −3.5 kV, the capillary voltage to −95 V, the tube lens voltage offset to −190 V, and the skimmer voltage to −46 V. Mass spectra were recorded from 250 to 1000 Th, with an AGC value of 5×10^5. All data were processed using the Qualbrowser application of Xcalibur version 2.1 (Thermo Fisher Scientific).

Plant Material. The roots of *G. africanum* were collected in Yaoundé (Centre Province, Cameron) in July 2006. A voucher specimen (accession number 21165/SFRK) has been deposited at the Cameroon National Herbarium of Yaoundé. The identification was confirmed by Mr. Victor Nana, Botanist of the Cameroon National Herbarium.

Extraction and Isolation. Dried and finely powdered roots of *G. africanum* (300 g) were defatted with toluene (2 L), extracted with 60% aqueous acetone (2 L; 2 times) at room temperature, and filtered. The filtrate was concentrated at 35 °C under reduced pressure. The aqueous residue was further partitioned between methyl *tert*-butyl ether (MTBE) and H_2O. The organic and aqueous extracts were concentrated and freeze-dried to yield 25.61 g (MTBE, **GaM**) and 28 g (H_2O, **GaA**), respectively.

To enhance the stilbenoid content, the aqueous-soluble partition (**GaA**, 20g) was prepurified on Amberlite XAD-7 (H_2O and acetone), using the published protocol.[19] This provided a semipurified extract enriched in the target molecules **1a** (0.1% w/w) and **1b** (0.03% w/w) with a purity higher than 95%, assessed by NMR and HPLC-DAD methods. The two compounds were purified from 2 g of this extract by combination of CPC using ternary biphasic system EtOAc/2-PrOH/H_2O (45:10:45, v/v) and preparative HPLC (see Supporting Information).

GaM was subjected to CPC using the quaternary biphasic Arizona system L with *n*-heptane/EtOAc/MeOH/H_2O (2:3:2:3, v/v) and preparative HPLC (see Supporting Information) to obtain the fractions containing compounds **2** (0.83% w/w), **3** (0.2% w/w), and **4** (0.2% w/w) with purity higher than 95%, assessed by NMR and HPLC-DAD.

*(7aS,8aS)-Gnemonoside A (**1a**):* white, amorphous powder; $[\alpha]^{20}_D$ −65 (*c* 0.3, MeOH); ^{1}H and ^{13}C NMR spectroscopic data, see Supporting Information, Table S1; HRESIMS $[M - H]^-$ *m/z* 777.2401.

*(7aR,8aR)-Gnemonoside A (**1b**):* white, amorphous powder; $[\alpha]^{20}_D$ −32 (*c* 0.2, MeOH); ^{1}H and ^{13}C NMR spectroscopic data, see Supporting Information, Table S1; HRESIMS $[M - H]^-$ *m/z* 777.2402.

*Gnemonoside C (**2**):* white, amorphous powder; $[\alpha]^{20}_D$ −40 (*c* 0.2, MeOH); ^{1}H and ^{13}C NMR spectroscopic data, see Supporting Information, Table S1; ESIMS $[M - H]^-$ *m/z* 615.

*Gnemonoside D (**3**):* white, amorphous powder; $[\alpha]^{20}_D$ −49 (c 0.1, MeOH); ^{1}H and ^{13}C NMR spectroscopic data, see Supporting Information, Table S1; ESIMS $[M - H]^-$ *m/z* 615.

*Gnetin C (**4**):* white, amorphous powder; $[\alpha]^{20}_D$ −1 (*c* 0.1, MeOH); ^{1}H and ^{13}C NMR spectroscopic data, see Supporting Information, Table S1; ESIMS $[M - H]^-$ *m/z* 453.

Enzymatic Hydrolysis of 1a and 1b. Separate solutions of **1a** (20 mg) and **1b** (20 mg) in H_2O, adjusted to pH 6.0 with 0.1 N NaOH, were treated with β-glucosidase (EC 3.2.1.21 Sigma) (1 mg/mL) for 14 h at 40 °C. Each solution was extracted with EtOAc three times. The EtOAc extracts were evaporated and purified by preparative HPLC to afford the two enantiomers of gnetin C (−)-**4**, $[\alpha]^{20}_D$ −17 (*c* 0.1, MeOH), MeOH) and (+)-**4**, $[\alpha]^{20}_D$ +20 (*c* 0.1, MeOH).

VCD Measurements. IR and VCD spectra were recorded with a ThermoNicolet Nexus 670 FTIR spectrometer equipped with a VCD optical bench.[22] In this optical bench, the light beam was focused by a BaF_2 lens (191 mm focal length) to the sample, passing an optical filter (depending on the studied spectral range), a BaF_2 wire grid polarizer (Specac), and a ZnSe photoelastic modulator (Hinds Instruments, type II/ZS50). The light was focused by a ZnSe lens (38.1 mm focal length) onto a 1 × 1 mm^2 HgCdTe (ThermoNicolet, MCTA* E6032) detector. IR and VCD spectra were recorded at a resolution of 4 cm^{-1} by coadding 50 and 36 000 scans (12 h acquisition time), respectively. The sample was held in a fixed path length (100 μm) cell with BaF_2 windows. IR and VCD spectra of the two enantiomers of gnetin C (obtained from the hydrolysis of **1a** and **1b**) were measured in DMSO-d_6 at a concentration of 50 mM. Additional IR and VCD spectra of natural gnetin C (**4**) and of compounds **1a**, **1b**, **2**, and **3** were recorded under the same experimental conditions. In all experiments, the photoelastic modulator was adjusted for a maximum efficiency at 1400 cm^{-1}. Calculations were done with the standard ThermoNicolet software, using Happ and Genzel apodization, de-Haseth phase-correction, and a zero-filling factor of 1. Calibration spectra were recorded using a birefringent plate (CdSe) and a second BaF_2 wire grid polarizer, according to a published procedure.[23] Finally, the solvent absorption was subtracted out in the presented IR spectra.

DFT Calculations. Calculation of the IR and VCD spectra began with conformational analyses of the 7a*S*8a*S* and 7a*R*8a*S* diastereomers of gnetin C. This involved exploring the entire conformational energy surface of the molecule and carrying out semiempirical RM1[24] calculations with the simulated annealing technique,[25] as both implemented in the package Ampac,[26] of the relative energies of conformers found in the various local minima of this surface. Energy minima were sought in two stages: (i) a nonlocal search focused on nine dihedral angles corresponding to hydroxy groups (5), to the rotations of the two phenyl rings linked to the benzofuran group (2), and to the rotations around the C═C bond (2) and (ii) a local energy relaxation of the whole degrees of freedom for each of the minima collected at stage (i). Twenty conformers within roughly 2.4 kJ/mol of the lowest energy conformer were kept for further DFT calculations.

The geometry optimizations, vibrational frequencies, absorption, and VCD intensities were calculated with the Gaussian 09 program[27] on the DELL cluster of the MCIA computing center at the University of Bordeaux. Calculations of the optimized geometry of about 20 conformers of (7a*S*,8a*S*)- and (7a*R*,8a*S*)-gnetin C were performed at the density functional theory level using the B3PW91 functional and the 6-31G** basis set. Vibrational frequencies, IR, and VCD intensities were calculated at the same level of theory, using the magnetic field perturbation method with gauge-invariant atomic orbitals.[28] The spectra were calculated for the isolated molecule in vacuo. For comparison with the experiment, the calculated frequencies were scaled by 0.962 and the calculated intensities were converted to Lorentzian bands with a half-width of 7 cm^{-1}.

Antiamyloidogenic Activity. Aβ (25−35) peptide was purchased from Bachem California (Torrance, CA, USA) and used without further purification. The GSNKGAIIGLM sequence of Aβ (25−35) peptide corresponds to residues of the human wild-type sequence Aβ (1−40). Curcumin was purchased from Bachem (Germany). A 1 mM stock solution of Aβ (25−35) peptide was prepared by solubilizing the lyophilized Aβ peptide upon brief vortexing in sterile H_2O at 4 °C, followed by sonication for 1 min. This peptide stock solution was aliquoted and stored at −20 °C. All subsequent steps were carried out at 4 °C to prevent any Aβ peptide polymerization. Stilbenes were solubilized in MeOH (i.e., stock solution of 1 mg/mL, then diluted to reach a 10 μM final concentration; aliquots were stored at −20 °C) and added to a solution of phosphate buffer (10 mM final concentration, pH 7.2) and Aβ peptide [100 μM concentration for Aβ (25−35)]. Typical experiments were carried out on a reaction mixture containing 80 μL of the phosphate buffer solution, 10 μL of the Aβ peptide solution, and 10 μL of MeOH without or with polyphenol. Sonication was performed for 5 min to avoid peptide aggregation as much as possible at time *t* = 0 h. The inhibiting effect of stilbenes was compared to that of curcumin as reference. Measurement of inhibitory activity was performed by UV−visible spectroscopy. UV−visible spectroscopic analyses were performed on a Cary 300 Bio UV−visible spectrophotometer (Varian, USA), and polymerization kinetics

dx.doi.org/10.1021/np500427v | J. Nat. Prod. XXXX, XXX, XXX−XXX

were monitored at 200 nm (i.e., peptide bond absorbance wavelength) for 6 h for the Aβ (25−35) peptide. We typically used six samples respectively containing Aβ peptide alone, stilbenes alone, a curcumin/Aβ peptide mixture, and three stilbene/Aβ peptide mixtures. The sample with stilbene alone was used to check that it had no influence on the absorbance, while the curcumin/Aβ peptide mixture was used as amyloid inhibitor control. A minimum of three independent measurements were carried out for each experiment.

■ ASSOCIATED CONTENT

Ⓢ Supporting Information

Additional information on the extraction of compounds **1**−**4**. ^{1}H and ^{13}C NMR data of stilbenoids **1**−**4** in CD_3OD. LC-ESI-FTMS of **1a** and **1b**. ^{1}H, ^{1}H−^{1}H COSY, ^{1}H−^{1}H ROESY, HSQC, and HMBC spectra of **1a**. VCD spectra of **1a**, **2**, and **3**. This material is available free of charge via the Internet at http://pubs.acs.org.

■ AUTHOR INFORMATION

Corresponding Authors

*E-mail: t.buffeteau@ism.u-bordeaux1.fr.

*Tel: +33-55-757-5955. Fax: +33-55-757-5952. E-mail: pierre.waffoteguo@u-bordeaux2.fr.

Notes

The authors declare no competing financial interest.

■ ACKNOWLEDGMENTS

This research was financially supported by the French Ministry of Research and the Aquitaine Regional Government. NMR experiments were performed at the Plateforme Métabolome-Fluxome, Centre de Génomique Fonctionnelle de Bordeaux, Bordeaux, France. The authors thank G. Fondeville for technical assistance and R. Cooke for proofreading the manuscript.

■ REFERENCES

(1) Hladik, C. M.; Hladik, A.; Linares, O. F. *Tropical Forests, People and Food: Biocultural Interactions and Applications to Development*; Parthenon Pub Group, 1993.

(2) Shiembo, P. N. In *Non-wood Forest Products of Central Africa: Current Research Issues and Prospects for Conservation and Development*; Based on the Outcome of the International Expert Meeting on Non-Wood Forest Products in Central Africa; FAO, 1999.

(3) Ali, F.; Assanta, M. A.; Robert, C. *J. Med. Food* **2011**, *14*, 1289−1297.

(4) Isong, E. U.; Adewusi, S. A. R.; Nkanga, E. U.; Umoh, E. E.; Offiong, E. E. *Food Chem.* **1999**, *64*, 489−493.

(5) Prakash, S.; Ahmed, J.; Zaman, A. *Phytochemistry* **1981**, *20*, 1455−1456.

(6) Lins, A. P.; Ribeiro, M. N. D. S.; Gottlieb, O. R.; Gottlieb, H. E. *J. Nat. Prod.* **1982**, *45*, 754−761.

(7) Ouabonzi, A.; Bouillant, M. L.; Chopin, J. *Phytochemistry* **1983**, *22*, 2632−2633.

(8) Shen, T.; Wang, X.-N.; Lou, H.-X. *Nat. Prod. Rep.* **2009**, *26*, 916−935.

(9) Rivière, C.; Pawlus, A. D.; Mérillon, J.-M. *Nat. Prod. Rep.* **2012**, *29*, 1317−1333.

(10) Jang, M.; Cai, L.; Udeani, G. O.; Slowing, K. V.; Thomas, C. F.; Beecher, C. W.; Fong, H. H.; Farnsworth, N. R.; Kinghorn, A. D.; Mehta, R. G.; Moon, R. C.; Pezzuto, J. M. *Science* **1997**, *275*, 218−220.

(11) Neafsey, E. J.; Collins, M. A. *Neuropsychiatr. Dis. Treat.* **2011**, *7*, 465−484.

(12) Rivière, C.; Papastamoulis, Y.; Fortin, P.-Y.; Delchier, N.; Andriamanarivo, S.; Waffo-Téguo, P.; Kapche, G. D. W. F.; Amira-Guebalia, H.; Delaunay, J.-C.; Mérillon, J.-M.; Richard, T.; Monti, J.-P. *Bioorg. Med. Chem. Lett.* **2010**, *20*, 3441−3443.

(13) Richard, T.; Poupard, P.; Nassra, M.; Papastamoulis, Y.; Iglésias, M.-L.; Krisa, S.; Waffo-Teguo, P.; Mérillon, J.-M.; Monti, J.-P. *Bioorg. Med. Chem.* **2011**, *19*, 3152−3155.

(14) Freedman, T. B.; Cao, X.; Dukor, R. K.; Nafie, L. A. *Chirality* **2003**, *15*, 743−758.

(15) Asai, T.; Taniguchi, T.; Yamamoto, T.; Monde, K.; Oshima, Y. *Org. Lett.* **2013**, *15*, 4320−4323.

(16) Manriquez-Torres, J. J.; Torres-Valencia, J. M.; Velazquez-Jimenez, R.; Valdez-Calderon, A.; Alvarado-Rodriguez, J. G.; Cerda-Garcia-Rojas, C. M.; Joseph-Nathan, P. *Org. Lett.* **2013**, *15*, 4658−4661.

(17) Bustos-Brito, C.; Sanchez-Castellanos, M.; Esquivel, B.; Calderon, J. S.; Calzada, F.; Yepez-Mulia, L.; Hernandez-Barragan, A.; Joseph-Nathan, P.; Cuevas, G.; Quijano, L. *J. Nat. Prod.* **2014**, *77*, 358−363.

(18) Iliya, I.; Tanaka, T.; Furasawa, M.; Ali, Z.; Nakaya, K.-I.; Iinuma, M.; Shirataki, Y.; Murata, J.; Darnaedi, D. *Heterocycles* **2001**, *55*, 2123−2130.

(19) Bisson, J.; Poupard, P.; Pawlus, A. D.; Pons, A.; Darriet, Ph.; Mérillon, J.-M.; Waffo-Téguo, P. *J. Chromatogr. A* **2011**, *1218*, 6079−6084.

(20) La Torre, G. L.; Laganà, G.; Bellocco, E.; Vilasi, F.; Salvo, F.; Dugo, G. *Food Chem.* **2004**, *85*, 259−266.

(21) Rivière, C.; Richard, T.; Quentin, L.; Krisa, S.; Mérillon, J.-M.; Monti, J.-P. *Bioorg. Med. Chem.* **2007**, *15*, 1160−1167.

(22) Buffeteau, T.; Lagugné-Labarthet, F.; Sourrisseau, C. *Appl. Spectrosc.* **2005**, *59*, 732−745.

(23) Nafie, L. A.; Vidrine, D. W. In *Fourier Transform Infrared Spectroscopy*; Ferraro, J. R.; Basile, L. J., Eds.; Academic Press: New York, 1982; Vol. 3, pp 83−123.

(24) Rocha, G. B.; Freire, I. O.; Simas, A. M.; Stewart, J. J. P. *J. Comput. Chem.* **2006**, *27*, 1101−1111.

(25) Bockisch, F.; Liotard, D.; Rayez, J. C.; Duguay, B. *Int. J. Quantum Chem.* **1992**, *44*, 619−642.

(26) *AMPAC-8*; Semichem: Shawnee, KS, 2004.

(27) Frisch, M. J.; Trucks, G. W.; Schlegel, H. B.; Scuseria, G. E.; Robb, M. A.; Cheeseman, J. R.; Scalmani, G.; Barone, V.; Mennucci, B.; Petersson, G. A.; Nakatsuji, H.; Caricato, M.; Li, X.; Hratchian, H. P.; Izmaylov, A. F.; Bloino, J.; Zheng, G.; Sonnenberg, J. L.; Hada, M.; Ehara, M.; Toyota, K.; Fukuda, R.; Hasegawa, J.; Ishida, M.; Nakajima, T.; Honda, Y.; Kitao, O.; Nakai, H.; Vreven, T.; Montgomery, J. A., Jr.; Peralta, J. E.; Ogliaro, F.; Bearpark, M.; Heyd, J. J.; Brothers, E.; Kudin, K. N.; Staroverov, V. N.; Kobayashi, R.; Normand, J.; Raghavachari, K.; Rendell, A.; Burant, J. C.; Iyengar, S. S.; Tomasi, J.; Cossi, M.; Rega, N.; Millam, N. J.; Klene, M.; Knox, J. E.; Cross, J. B.; Bakken, V.; Adamo, C.; Jaramillo, J.; Gomperts, R.; Stratmann, R. E.; Yazyev, O.; Austin, A. J.; Cammi, R.; Pomelli, C.; Ochterski, J. W.; Martin, R. L.; Morokuma, K.; Zakrzewski, V. G.; Voth, G. A.; Salvador, P.; Dannenberg, J. J.; Dapprich, S.; Daniels, A. D.; Farkas, Ö.; Foresman, J. B.; Ortiz, J. V.; Cioslowski, J.; Fox, D. J. *Gaussian 09*, revision A.1; Gaussian Inc.: Wallingford, CT, 2009.

(28) Cheeseman, J. R.; Frisch, M. J.; Delvin, F. J.; Stephens, P. J. *Chem. Phys. Lett.* **1996**, *252*, 211−220.